

Superconducting wires of Cu-Nb₃Sn: the liquid-phase sintering method

OSCAR F. DE LIMA*, ABSAIR T. DE REZENDE
Instituto de Física, UNICAMP, 13100 Campinas, São Paulo, Brazil

A new method aimed at obtaining Cu-Nb₃Sn wires in a simple and low cost way is introduced. A powder mixture of Cu-30 wt % (Nb-H)-0.3 wt % Al was degassed and heat treated ($T = 1200^\circ\text{C}$) under vacuum, leading to soft, highly dense Cu-Nb sintered samples. Tin diffusion and reaction resulted from external and internal processes. In the latter case cores of tin-rich alloy were used, but an intrinsic drawback related to the occurrence of hard η -phase precipitates can be identified. The critical temperature, critical current density, and normal electrical resistivity at 19 K are analysed and correlated with the other parameters (e.g. reaction time and Cu/SC ratio).

1. Introduction

Superconducting wires of Cu-Nb₃Sn are very attractive owing to their ability to transport very high electrical currents under high magnetic fields ($> 10\text{ T}$). The production of this wire by the conventional bronze method [1, 2] is technologically complicated, requiring several intermediate annealing steps in order to recover the bronze matrix ductility. However, until now this has been the usual commercial process, although very expensive.

During the last ten years several alternative techniques [3] have appeared, aiming to produce Nb₃Sn wires through a simpler and less expensive way, and also preserving the same, or better, wire characteristics found with the conventional method. The *in situ* [4] and powder-metallurgical (P/M), hot [5] and cold [6], methods have been extensively studied [3] and they are promising for commercial scale-up. These new methods present some common features:

1. The first step of preparation consists in obtaining small niobium particles uniformly dispersed throughout the copper matrix. This is accomplished by rapidly quenching a Cu-Nb liquid mixture ($T \sim 1800^\circ\text{C}$) for the *in situ* method, and by consolidating a mixture of copper and niobium powders in the case of P/M methods;

2. The final wires, have discontinuous niobium (or Nb₃Sn, after reaction) filaments embedded in a copper matrix (with residual tin, after reaction). These filaments result from elongation of the initial niobium particles, during the deformation work;

3. High critical currents are possible because of percolation and proximity effects between the superconducting filaments [3].

There are several inherent advantages of P/M processing over other methods [7] mainly owing to its versatility and convenience for processing large amounts of material. However, the presence of adsorbed oxygen at the powder surface, prior to

elongation of the niobium particles, constitutes a serious problem. Even at low concentrations of oxygen (e.g. 0.6 at % O) [8] the ductility of niobium is severely reduced. To overcome this problem two alternatives were tested:

1. Addition of a third element (e.g. aluminium, zirconium, hafnium, magnesium, calcium) to reduce the oxygen, in the hot P/M method (extrusion at $T \sim 1000^\circ\text{C}$) [5]; and

2. Deformation of the Cu-Nb powder mixture at low temperature ($< 500^\circ\text{C}$) in order to avoid oxygen diffusion into niobium, in the cold P/M method [6, 7]. In this case, high quality soft niobium powder ($< 0.2\text{ at } \% \text{ O}$) is required.

In the present paper a new method is presented aimed at obtaining Cu-Nb₃Sn wires in a simple and relatively low cost way. We use, for the first time, Nb-H powder instead of niobium powder, and also liquid-phase sintering ($T = 1200^\circ\text{C}$), in order to prepare the initial Cu-Nb sample [9] yielding several advantages with respect to the previous methods.

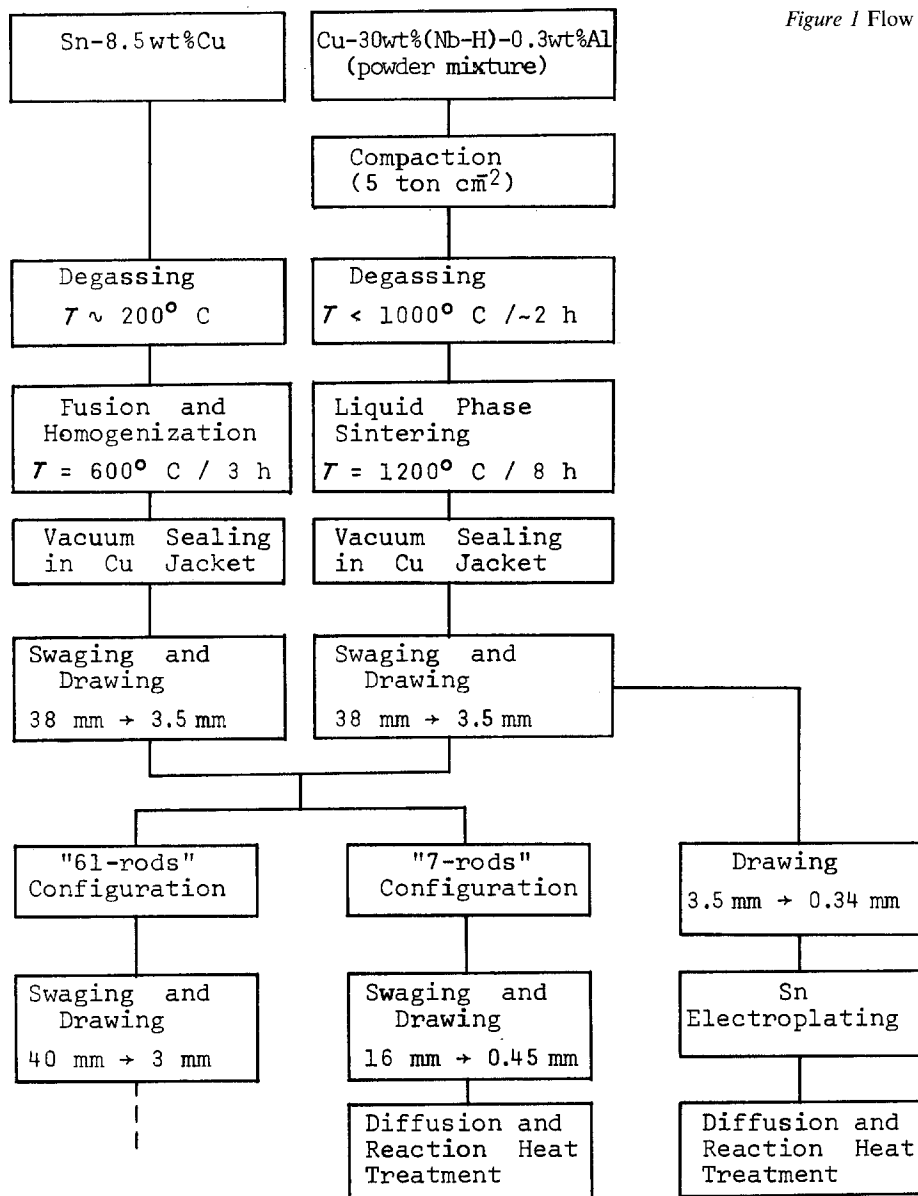
2. Sample preparation and microstructure

Fig. 1 outlines the various steps required to produce the Cu-Nb₃Sn wire. Initially the powders, having particle sizes in the range between 149 and 297 μm , were mixed with a composition of Cu-30 wt % (Nb-H)-0.3 wt % Al. Copper and aluminium powders were of commercial quality ($\sim 99.5\%$ purity). The Nb-H powder was prepared by doping niobium sheets (99.9% purity) under 1 atm H₂, with temperature varying from 800°C down to 300°C, followed by milling and sizing. The use of Nb-H powder in substitution to the commonly used niobium powder [3, 5-7, 9] has the following advantages:

1. The oxygen content in Nb-H powders ($\sim 750\text{ wt p.p.m.}$) was found to be nearly one-half lower than for the degassed niobium powders

* Present address: Argonne National Laboratory, MST-223, 9700 S. Cass Ave., Argonne, Illinois 60439, USA.

Figure 1 Flow chart of the wire preparation method.



(~ 1300 wt p.p.m.), in the range 149 to 297 μm used in this work;

2. The hydrogen released during the sintering heat treatment (under vacuum) acts as a reducing atmosphere and also an activation agent promoting the wetting between liquid copper and niobium [10], thus favouring sample densification [11, 12];

3. Energy and time are saved because the hydrogen degassing step is made *in situ*, simultaneously with the liquid-phase sintering heat treatment.

A small amount of aluminium (0.3 wt %) was added to guarantee the reduction of oxygen adsorbed at the surface of the niobium particles, which normally is not reduced by hydrogen [5]. In another study [10] some evidence was given for a new mechanism of oxygen reduction on niobium by hydrogen when in the presence of liquid copper. However, more work is under way in order to verify if, based on this mechanism, we can avoid completely the addition of aluminium.

The mixed powders (Cu-30 wt % (Nb-H)-0.3 wt % Al) were pressed in a stainless steel double piston, up to a pressure of 5 ton cm^{-2} . The compact

density was around 70% theoretical density which was equivalent to 8.7 g cm^{-3} . Each pressed sample was heat treated inside a quartz crucible, in an induction furnace, by heating progressively up to a temperature of 1200°C. Hydrogen is released almost completely during this heat treatment, and copper melts at 1090°C [13], the peritectic temperature of the Cu-Nb system. Holding $T = 1200^\circ\text{C}$ for 8 h, the liquid-phase sintering occurs under a final vacuum of 10^{-5} torr. The final hydrogen concentration was found to be lower than 100 at p.p.m. The Vickers microhardness was found to be around 130 kg mm^{-2} at the niobium particles, and around 91 kg mm^{-2} at the copper matrix.

Several samples of Cu-Nb were prepared (Fig. 2), all reaching a density around 8.3 g cm^{-3} (~95% theoretical density). They typically weighed 320 g and were of cylindrical shape, being 31 mm diameter and around 50 mm high.

Each Cu-Nb sample was inserted in a copper jacket having 38 mm outer diameter, vacuum sealed, and swaged down to 4.7 mm. Smaller diameters were obtained by drawing. We were able to produce long lengths of wires with 0.25 mm diameter, having

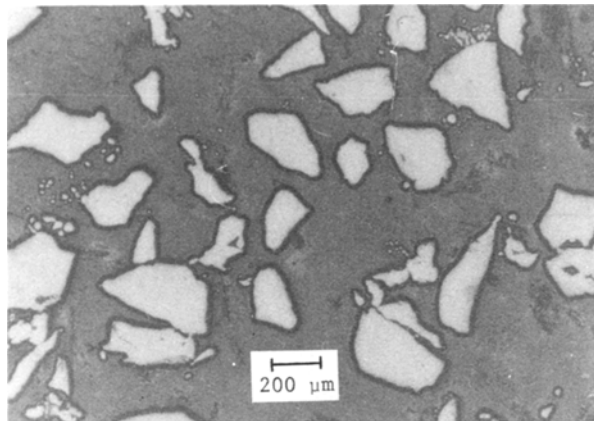


Figure 2 Typical microstructure of the sintered Cu-Nb samples.

excellent workability, without any rupture or intermediate heat treatments. The total areal reduction factor in this case was $A_0/A = 2.3 \times 10^4$.

Two methods were employed in order to introduce tin.

1. Internal diffusion, by inserting some rods of tin-rich alloy (Sn-8.5 wt % Cu) regularly distributed among the Cu-Nb rods, in a copper jacket. We have used two different hexagonal arrangements: (a) the “61-rods”, consisting of 48 Cu-Nb rods plus 13 Sn-Cu rods; (b) the “7-rods”, consisting of 6 Cu-Nb rods plus 1 Sn-Cu rod. These rods were 3.5 mm diameter and both arrangements were sealed under vacuum. The tin concentration with respect to niobium was around 40 wt % in both cases, the copper/superconductor (Cu/SC) ratio was around 8 (“7-rods”) and 5 (“6-rods”).

2. External diffusion, by electroplating the Cu-Nb wires of 0.34 mm diameter with tin in two steps, each followed by a diffusion heat treatment (220°C for 14 h → 300°C for 3 h → 500°C for 7 h), in order to avoid balling-up of the tin [14]. In this case we had around 36 wt % Sn with respect to niobium, and $Cu/SC = 2.3$.

The “61-rods” and “7-rods” arrangements were deformed by swaging and drawing until some ruptures began to appear, for wire diameters between 2.0 and 3.0 mm. However, small lengths (~1 m) of the “7-rods” wire, having 0.45 mm diameter, were obtained after careful work. The total areal reduction factor in this case is $A_0/A = 1.5 \times 10^5$ and the niobium filament density $3 \times 10^5 \text{ mm}^{-2}$.

The reaction heat treatment, leading to the Nb_3Sn Al5 phase formation, was done at 700°C, with the samples encapsulated inside quartz tubes under an argon atmosphere. Reaction times between 10 and 260 h were used. Partial tin diffusion was promoted previously through a step-wise heat treatment between 200 and 500°C.

Fig. 3 shows a polished transverse cross section of an unreacted “61-rods”, and Fig. 4 shows scanning electron micrographs (SEM) of the typical filamentary structure for the reacted “7-rods” wires, after being slightly etched by a solution of nitric acid. During the cold deformation step the niobium particles were elongated to filaments having a ribbon-like shape

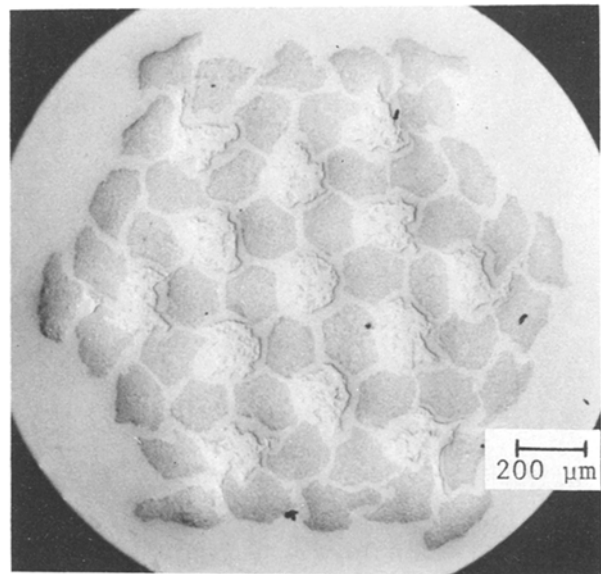


Figure 3 Transversal cross section view for a “61-rods” wire having 2.1 mm diameter. Clear cores, Sn-Cu rods; dark cores, Cu-Nb rods.

(Fig. 4b) due to a $\{110\}$ preferred texture which is developed for bcc materials [15].

2.1. Internal tin diffusion

Although not well understood, internal tin diffusion, by using tin rich (Sn-Cu) alloy cores, has been employed with increasing interest [16–19]. In our work we have detected an intrinsic drawback in this process, related to the presence of large precipitates of the intermetallic η -phase (Cu_6Sn_5). We have employed the commonly used Sn-8.5 wt % Cu alloy as the source of tin. This alloy was melted and homogenized under vacuum (10^{-3} torr) for 3 h at $T = 600^\circ\text{C}$ (Fig. 1). After furnace-cooling, the Vickers hardness was around 6.7 kg mm^{-2} , much lower than the Cu-Nb samples. By rapid cooling in a bath at 0°C , the hardness was increased to 15 kg mm^{-2} .

By using a special microetching solution type Sn-m2 ([20] p. 84), the η -phase was revealed as small dark precipitates (Fig. 5) regularly dispersed throughout the tin-rich eutectic matrix, as expected by the equilibrium phase diagram [21]. However, the Sn-Cu alloy microstructure was strongly different in the wires, after the mechanical deformation. Figs 6a and b show details of the Sn-Cu core for the “61-rods” and “7-rods” wires, respectively, after a treatment using the special microetching solution type Cu-m8 ([20] p. 60). In this case clear fields correspond to the η -phase and dark fields to the tin-rich matrix. This result was checked by measuring the Vickers microhardness, which gave around 320 kg mm^{-2} for the η -phase and around 15 kg mm^{-2} for the tin-rich matrix. During the deformation process the η -phase seems to be rearranged into large precipitates, accompanied by an increase in its volume fraction. A possible mechanism to explain these facts is perhaps the diffusion of certain amount of tin outside the core region, activated by the temperature rise caused by the mechanical work of deformation.

We believe that the hard precipitates of η -phase

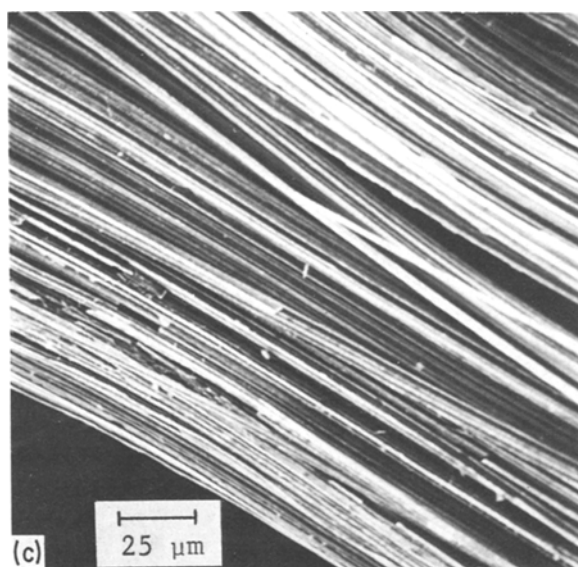
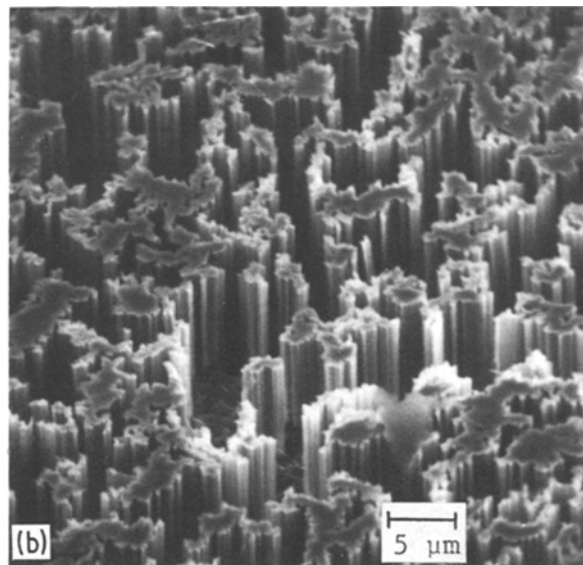
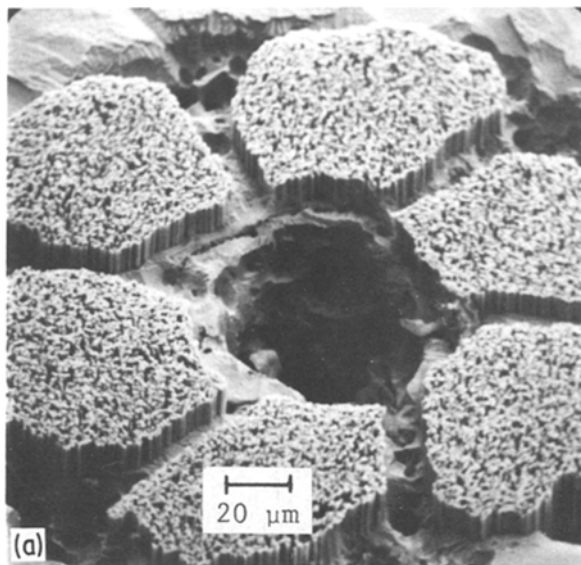


Figure 4 SEMs of typical filamentary structures for the reacted “7-rods” wires: (a) the six bundles of Nb₃Sn filaments with a density around $3 \times 10^5 \text{ mm}^{-2}$; (b) magnified detail of the ribbon-like shaped filaments; (c) longitudinal view of a deep etched wire.

dissolved in nitric acid. Then, the unattacked brittle filaments were milled to a fine powder which was analysed in the diffractometer.

Internal tin diffusion (“7-rods” wires) was found to be more effective, producing the complete reaction between niobium and tin after 260 h, and around 80% reaction after 10 h. For external diffusion wires nearly 15% Nb remained unreacted even after 260 h, and only 10% was reacted after 10 h. The Nb₃Sn lattice parameter for the full reacted samples varied between $0.5280 \pm 0.0005 \text{ nm}$ and $0.5285 \pm 0.0005 \text{ nm}$, within the expected homogeneity range for the A15 phase [22], although being slightly lower than the standard value (0.5289 nm) observed for samples having the correct stoichiometry (Nb–25 at % Sn).

were the intrinsic cause for the wire failure when drawing both kinds of arrangements as already mentioned. These hard precipitates must act as obstacles against the plastic flow of the tin-rich matrix, thus bringing the failure of the whole sample sooner. The Cu–Nb rods have shown a ductile fracture with necking (Fig. 7a), while a brittle fracture was occurring for the Sn–Cu rods. Fig. 7b is an enlarged view (SEM) of the fractured surface for a Sn–Cu rod, showing many small cavities, which contains some angular precipitates (η -phase).

Perhaps by using a simpler arrangement, like a drilled cylinder of Cu–Nb with inserted Sn–Cu rods, or by designing optimized conditions for deformation (die angle, drawing speed, reduction per step, etc.), it may be possible to successfully reduce the conjugated wires down to very fine diameters ($< 0.5 \text{ mm}$), without ruptures and intermediate anneals.

2.2. X-ray analysis

We have employed X-ray diffraction to check the degree of wire reaction by an independent and reliable means. Firstly, the copper matrix of the wires of Cu–Nb₃Sn annealed for 10 and 260 h was completely

3. Results and discussion

The critical temperature (T_c) for all samples was determined at the midpoint of the resistive transition ($S \rightarrow N$), by using the conventional four-probe method, with temperature being measured through a calibrated

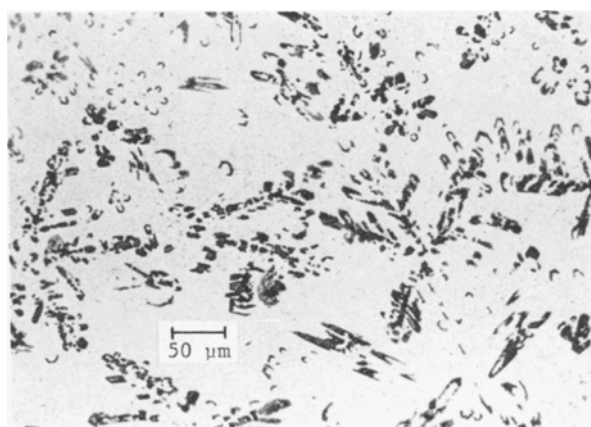


Figure 5 Typical microstructure of the as-cast Sn–8.5 wt % Cu alloy after a special microetching treatment. The η -phase is revealed as small dark precipitates dispersed throughout the tin-rich matrix.

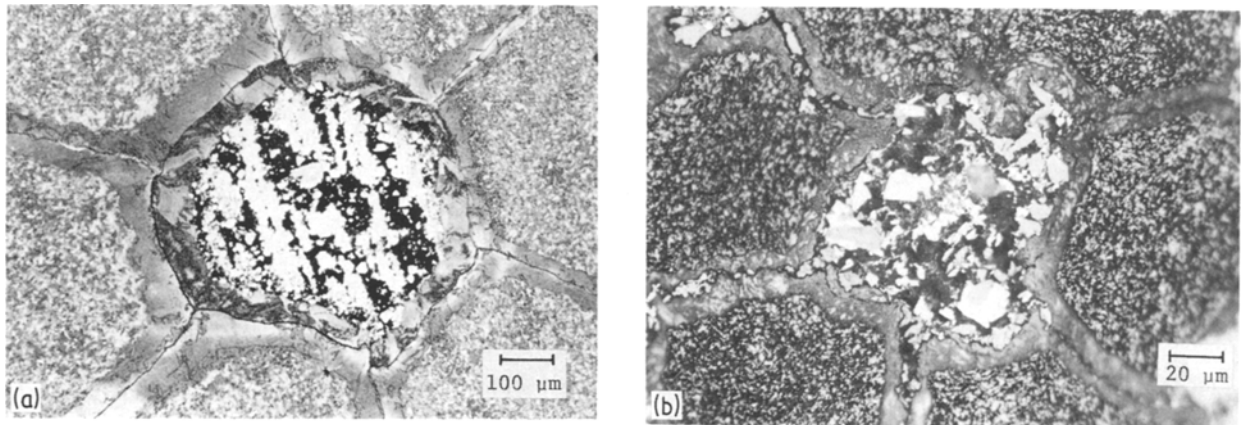


Figure 6 Microstructure of the transversal cross section showing details of the Sn–Cu core (centre) for (a) the “61-rods”, and (b) “7-rods” wires. Clear fields, η -phase; dark fields, tin-rich matrix.

carbon–glass resistor. The normal state resistivity (ρ_N), just above the transition ($T \sim 19$ K), was determined within 2% error. This error arises mainly from the distance measurements between the voltage leads, settled 20.0 mm apart. The overall critical current density (J_c) at transverse fields and $T = 4.2$ K were determined by the conventional four-probe method. A special sample holder made of fibreglass/epoxy (G-10) was employed in order to minimize the effects due to thermal contractions. The critical current was defined by the $1 \mu\text{V cm}^{-1}$ criterion, with the voltage leads being 10 mm apart.

The wires prepared by external tin diffusion were poorly stabilized, because of the relatively high electrical resistivity ($\sim 10^{-5} \Omega\text{cm}$) and degraded thermal conductivity of the matrix (residual bronze), leading to some abrupt transitions accompanied by sample melting. Therefore, a copper shunt was employed for the critical current measurements in these samples.

The values obtained for T_c , ρ_N and J_c (Figs 8 to 11) are averages taken over three samples for T_c and ρ_N (scattering lower than 1%), and two samples for J_c (scattering within 20%). All measured samples were 3 cm in length.

3.1. Effect of reaction time

T_c increases with reaction time for all samples, reaching a maximum plateau after about 150 h (Fig. 8). This behaviour accompanies the compositional variation of the A15 phase toward the correct stoichiometry [23]. We have also observed a consistent narrowing of the transition width, and an increase of the lattice parameter with reaction time.

The maximum T_c was around 16.80 ± 0.05 K for the external diffusion wires, and around 16.40 ± 0.05 K for the internal diffusion wires. These values are below the standard for the pure A15 phase (18.3 K), partially due to the effect of higher pre-stress in the bronze matrix, generated by differential thermal contractions occurring between the reaction temperature (700° C) and the measuring temperature (4.2 K) [2]. Based on this interpretation and using some phenomenological relations [2], the higher T_c values for the external diffusion wires can be explained through their lower Cu/SC ratio (2.3) with respect to the Cu/SC ratio for the external diffusion wires (8.0). Assuming the same intrinsic T_c^* for both types of wires and the parabolic relationship between $\Delta T_c = T_c^* - T_c$ and $R = \text{Cu/SC}$ [2]: $\Delta T_c \propto [R/(1 + R)]^2$, we can

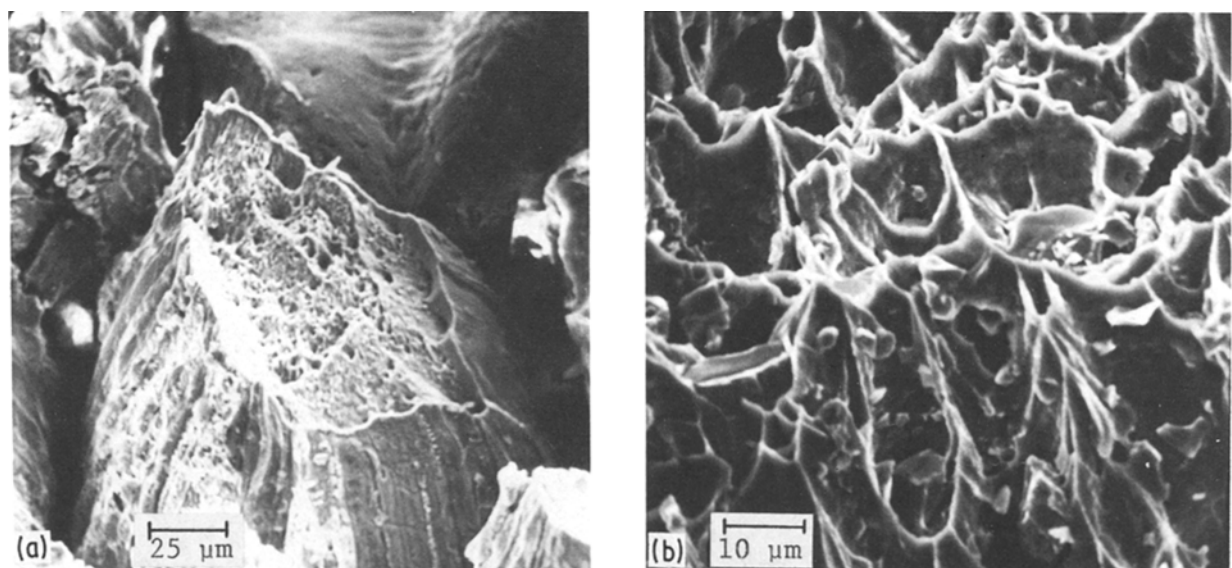


Figure 7 SEMs showing details of the fractured surface of a “7-rods” wire. (a) Ductile fracture of a Cu–Nb rod; (b) small cavities containing angular precipitates (η -phase) in a brittle fractured Sn–Cu rod.

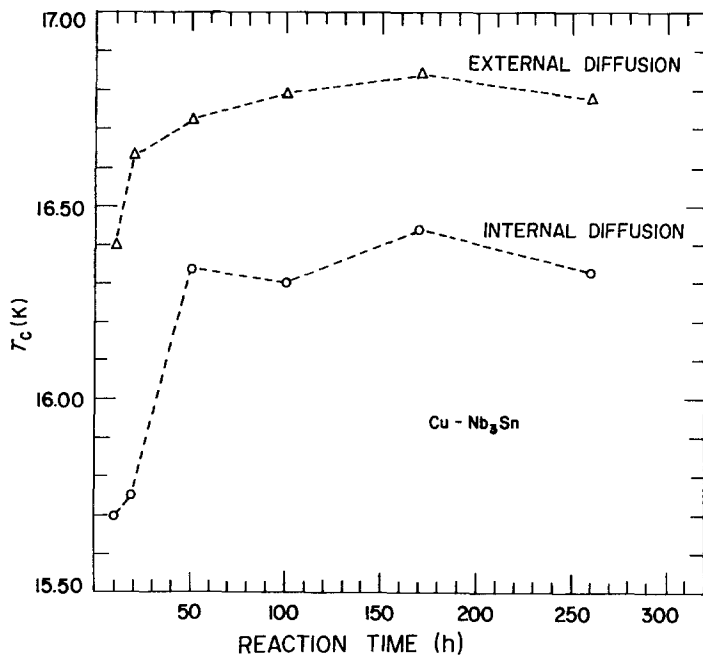


Figure 8 Critical temperature, T_c , plotted against reaction time. Reaction temperature: 700°C .

calculate:

$$\frac{\Delta T_c^{\text{ext}}}{\Delta T_c^{\text{int}}} = 0.6 \quad (1)$$

From Fig. 8:

$$\Delta T_c^{\text{int}} - \Delta T_c^{\text{ext}} = 0.4 \quad (2)$$

Combining Equations 1 and 2 we find $\Delta T_c^{\text{int}} = 1.0\text{ K}$ and $\Delta T_c^{\text{ext}} = 0.6\text{ K}$, in close agreement with previous data for wires having the same Cu/SC ratio and processed by the bronze method [2, 24]. On the other hand, the intrinsic T_c^* is found to be 17.4 K , being still lower than 18.3 K , probably due to the non-stoichiometric composition (as suggested by the X-ray data) and also some residual structural disorder [2].

The variation of ρ_N with reaction time (t) is mainly due to the tin content variation in the copper matrix. Therefore, the curves ρ_N against t (Fig. 9) could give some interesting information about tin diffusion and reaction kinetics. Initially ρ_N should increase because of the reduction of the electronic mean free path with the increasing tin content in the matrix. On the other hand, the reaction leading to the Nb_3Sn phase cleans the matrix by consuming tin, thus acting in the

opposite direction and lowering ρ_N . Therefore the competition between tin diffusion and reaction should determine the shape of the ρ_N against t curves. Moreover, owing to the limited tin content ρ_N should decrease after some time. This was observed after 170 h heat treatment (700°C) for the internal diffusion wires, but was not observed up to 260 h for the external diffusion wires. This result is consistent with the X-ray data, which have detected about 15 at % unreacted niobium for the latter case. The ρ_N values for internal diffusion wires were lower and experienced small relative variations due to its higher Cu/SC ratio which exceeds three times that for the external diffusion wires. This might explain why the external diffusion wires showed inferior stability during critical current measurements.

3.2. Critical currents

Fig. 10 (internal diffusion wires) and Fig. 11 (external diffusion wires) show preliminary results for the critical current density J_c under transverse magnetic fields up to 7 T. J_c increases systematically with increasing reaction times. However, for the internal diffusion wires it seems that J_c begins to decrease after 170 h, being apparently correlated with the completion of the

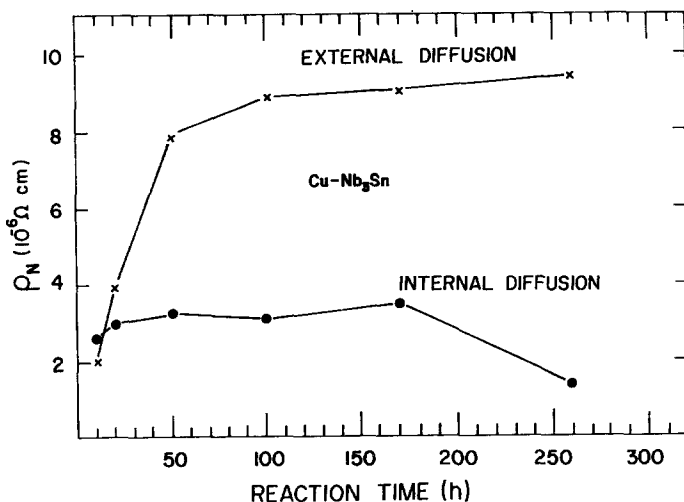


Figure 9 Normal electrical resistivity at 19 K, ρ_N , plotted against reaction time. Reaction temperature: 700°C .

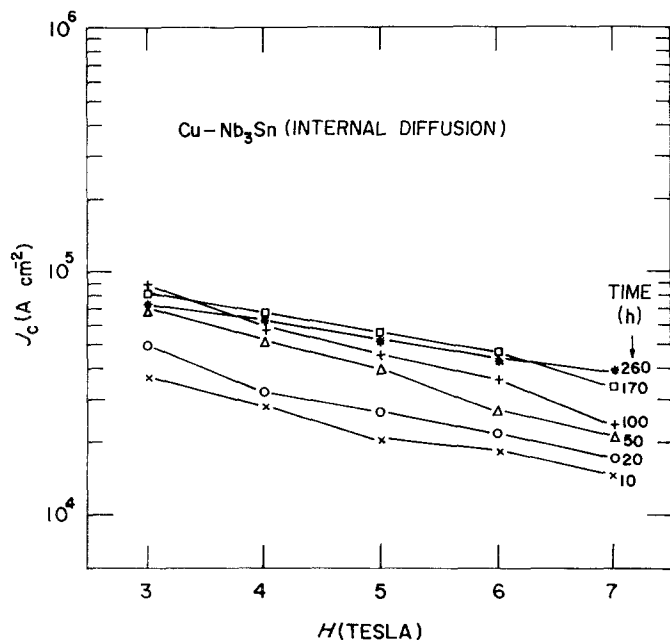


Figure 10 Overall critical current density, J_c , plotted against applied transverse field H for internal diffusion wires at different reaction times. $T = 4.2$ K.

Nb_3Sn reaction, as checked by X-rays for the 260 h samples. Therefore, after 170 h, the preponderant effect of Nb_3Sn grain growth should act negatively on J_c by lowering the volumetric pinning force due to grain boundaries [25].

Our present J_c values are not yet optimized. Even so, they are in the same range of typical optimized values found for Nb_3Sn wires prepared by the bronze method [26]. More work is being done in our laboratory and will be published in the future.

4. Conclusions

Many studies have been done in recent years towards new alternatives to produce $Cu-Nb_3Sn$ wires with good properties and lower costs compared with the bronze method. This paper presents a new method based on the liquid phase sintering of a $Cu-30$ wt % $(Nb-H)-0.3$ wt % Al powder mixture, followed by tin diffusion and reaction through external (electroplating) and internal ($Sn-Cu$ cores) processes. The main conclusions are:

1. The innovative use of $Nb-H$ powder has been demonstrated to be successful. Excellent mechanical properties and workability were obtained, in addition to the inherent lower costs than when using pure niobium powder.

2. Internal tin diffusion by using cores of the tin-rich $Sn-8.5$ wt % Cu alloy have an intrinsic drawback related to the presence of hard η -phase precipitates. This leads to brittle fracture when drawing the conjugated $(Cu-Nb)/(Sn-Cu)$ wires to diameters lower than 3 mm.

3. T_c was around 16.8 K for the external diffusion wires and around 16.4 K for the internal diffusion wires. Degradation due to the pre-stress effect of the matrix upon T_c was estimated to be $\Delta T = 1.0$ K (internal diffusion wires), and $\Delta T_c = 0.6$ K (external diffusion wires), being correlated with the Cu/Sn ratio.

4. The electrical resistivity at $T = 19$ K and the X-ray data have indicated that tin diffusion and reaction ($T = 700^\circ C$) were faster for the internal diffusion

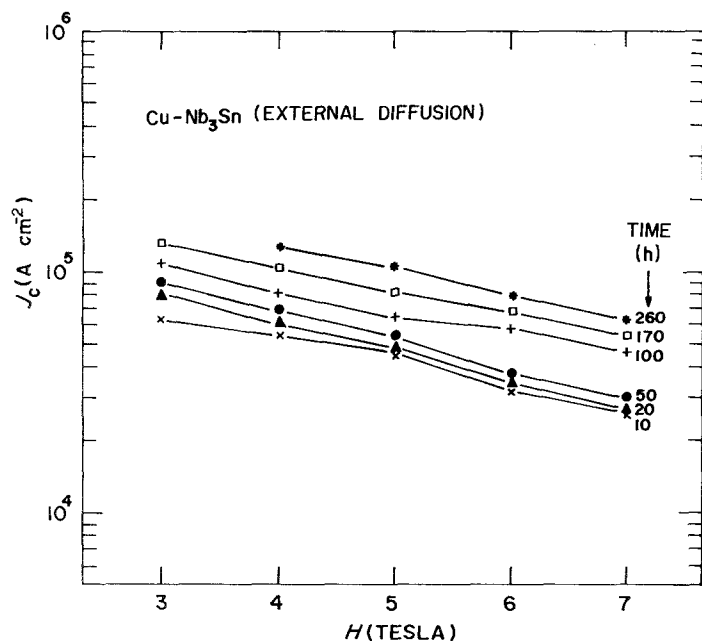


Figure 11 Overall critical current density, J_c , against applied transverse field, H , for external diffusion wires at different reaction times. $T = 4.2$ K.

wires. These wires were completely reacted after 260 h, while around 15 at % Nb remained unreacted in the external diffusion wires for this same time.

5. J_c values under transverse magnetic fields are not yet optimized. However, the best values, around 10^5 A cm^{-2} at $H = 7 \text{ T}$, are in the same range of optimized values for wires prepared by the bronze method.

Acknowledgements

The authors are grateful to the following people for their help in this research: Mr J. Outubo, Pirelli Co (deformation work); Mr J. A. P. Neto (critical current measurements); Dr K. Kaltembach, Dr S. Gama and Mr J. C. Petoilho (metallography); Miss Rita H. B. Jacon (SEMs); Dr Grallath and Dr K. Schultze, Max-Planck-Institut, Stuttgart (purity analysis of the powders); Dr S. Moehlecke for many valuable discussions, and Dr M. B. Brodsky for reading the manuscript. This work was partially supported by the Fundacao de Tecnologia Industrial – STI/MIC – Brazil. One of the authors (O.F.L.) acknowledges the financial support from FAPESP, through contract No. 85/0849-4.

References

1. A. R. KAUFMAN and J. J. PICKETT, *Bull. Am. Phys. Soc.* **15** (1970) 833.
2. M. SUENAGA, in "Superconductor Materials Science, Metallurgy, Fabrication, and Applications", edited by S. Foner and B. B. Schwartz (Plenum, New York, 1981) p. 201.
3. R. ROBERGE, *ibid.*, p. 389.
4. C. C. TSUEI, *Science* **180** (1973) 57.
5. R. BORMANN, H. C. FREYHARDT and H. BERGMANN, *Appl. Phys. Lett.* **35** (1979) 944.
6. R. FLÜKIGER, S. FONER, E. J. McNIFF Jr and B. B. SCHWARTZ, *Appl. Phys. Lett.* **34** (1979) 763.
7. R. FLÜKIGER, R. AKIHAMA, S. FONER, E. J. McNIFF Jr and B. B. SCHWARTZ, in "Advances of Cryogenic Engineering Materials", Vol. 26, edited by A. F. Clark and R. P. Reed (Plenum, New York, 1980) p. 337.
8. H. SHIRAIISHI, K. FURUYA and R. WATANABE, *J. Less-Common Met.* **63** (1979) 147.
9. O. F. de LIMA, in Proceedings of the 2nd Japan-Brazil Symposium, Rio de Janeiro, October (1980) (Internal Report S-060/80, Instituto de Fisica, Unicamp, Campinas, Brazil, 1980).
10. O. F. de LIMA, M. KREHL and K. SCHULZE, *J. Mater. Sci.* **20** (1985) 2464.
11. K. V. SEBASTIAN and G. S. TENDOLKAR, *Powder Met. Int.* **11** (1979) 62.
12. W. J. HUPPMANN, H. RIEGGER, W. A. KAYSER, V. SMOLEJ and S. PEJONIK, *Z. Metallkde* **70** (1979) 707.
13. C. ALLIBERT, J. DROILLE and E. BONNIER, *Compt. Rend.* **268** (1969) 2277.
14. J. D. VERHOEVEN, E. D. GIBSON and C. C. CHENG, *Appl. Phys. Lett.* **40** (1982) 87.
15. J. BEVK, J. P. HARBISON and J. L. BELL, *J. Appl. Phys.* **49** (1978) 6031.
16. Y. HASHIMOTO, K. YOSHIZAKI and M. TANAKA, in Proceedings of 5th International Cryogenic Engineering Conference, Kyoto, Japan edited by K. Mendelsohn (IPC Busihers Press, Guildford, UK, 1974) p. 332.
17. Y. KOIKE, H. SHIRAKI, S. MURASE, E. SUZUKI and M. ICHARA, *Appl. Phys. Lett.* **29** (1976) 384.
18. W. G. MARANCIK, E. ADAM, E. GREGORY and M. SUENAGA, *IEEE Trans. Mag.* **MAG-19** (1983) 910.
19. H. ZHANG, S. POURRAHIMI, J. OUTUBO, C. L. THIEME, B. B. SCHWARTZ and S. FONER, *ibid.* **MAG-19** (1983) 769.
20. G. PETZOW, "Metallographic Etching" (American Society for Metals, Metals Park, Ohio, 1978) p. 84.
21. M. HANSEN, "Constitution of Binary Alloys", 2nd Edn, (McGraw-Hill, New York, 1958) p. 633.
22. V. G. KUZNETSOVA, V. A. KOVALEVA and A. V. BEZNOSIKOVA, in "Physics and Metallurgy of Superconductors", edited by E. M. Savitskii and V. V. Baron (Consultants Bureau, New York, 1970) p. 167.
23. S. MOEHLECKE, PhD thesis, University of Campinas, Brazil (1977).
24. T. S. LUHMAN and M. SUENAGA, *Appl. Phys. Lett.* **129** (1976) 61.
25. R. M. SCANLAN, W. A. FIETZ and E. F. KOCK, *J. Appl. Phys.* **46** (1975) 2244.
26. H. HILLMANN, H. KUCKUCK, E. SPRINGER, H. J. WEISSE, M. WILHELM and K. WOHLLEBEN, *IEEE Trans. Mag.* **MAG-15** (1979) 205.

Received 12 September
and accepted 14 October 1985